Effect of Barium doped Zirconium Dioxide Nanoparticlesby Co-precipitation Method and their Photocatalytic Activities

S.Jeba Jenifa[1], B.Helina[2*]
[1]Research Scholar
Department of Physics
St. Xavier's College (Autonomous), Palayamkottai – 627 002
Affiliated to ManonmaniumSundaranar University, Tirunelveli – 627002, Tamilnadu, India.
[2]Assistant Professor of Physics
Department of Physics
St. Xavier's College (Autonomous), Palayamkottai – 627 002
Affiliated to ManonmaniumSundaranar University, Tirunelveli – 627002, Tamilnadu, India.
E-Mail: helinafredy@gmail.com

Abstract:

Zirconium dioxide nanoparticles were synthesized in the current study using Co-precipitation technique. The Zirconium (IV) oxynitrate hydrate ($ZrN_2O_7.xH_2O$) aqueous solution was treated by adding ammonia solution at ambient temperature to produce Zirconium dioxide nanoparticles. And addition of barium in two different weight percentage also produced barium doped Zirconium dioxide nanoparticles. Some characterization methods were used to examine the synthesized nanoparticles. The structural, morphological, optical, electrochemical and catalytic properties of the prepared samples were studied. XRD analysis of synthesized ZrO_2 nanoparticles revealed that they are tetragonal in structure. Their crystallite sizes are increased first then decreased when increasing doping concentration. From SEM images, the surface morphology of synthesized nanoparticlesare observed as spherical and some irregular clusters. EDAX spectrashow the presence of Zr, O and Ba elements with high purity in the prepared nanoparticles. From UV studies, the cutoff wavelength is obtained from the absorption spectra. FromTauc's plot the band gap energies were calculated in increasing order. FTIR spectroscopy confirmed the presence of tetragonalZrO_2. The formation of tetragonal structure of ZrO_2 is confirmed by the peak obtained in Raman spectroscopy. Photoluminescence spectra provide evidence of defects and the charge carrier recombination process. Increasing intensity shows the increasing recombination process. In photocatalytic activities, the excess amount of charge carrier increases the photocatalytic degradation of Rhodamine B dye when barium doping concentration is increased.

DOINumber: 10.48047/NQ.2022.20.9.NQ44935 **NeuroQuantology2022;20(9): 8044-8061**

1. INTRODUCTION:

Zirconium Dioxide, also known asZrO_2, is well-known for a number of characteristics, including non-toxicity, eco-friendliness, thermal stability, high corrosion resistance, superplastic deformation, microbial resistance, increased fracture toughness, optical and electrical properties, a surface area more specialized in nature and photocatalyst activity [1]. It is possible to make zirconium inorganic and organic substances using zirconium metal. The simple production of ZrO_2 in nanoscale proportions has grown recently due to its increased use [2]. ZrO_2 nanoparticles can be produced using a variety of techniques, likesono-chemical, hydrolysis, sol-gel, hydrothermal, microwave, spray pyrolysis, vapour phase and precipitation.ZrO_2 occurs naturally in three variable forms: monoclinic [m-ZrO_2], tetragonal [t-ZrO_2] and cubic [c-ZrO_2] at various temperatures and in normal atmospheres [2-5]. The m-ZrO_2 phase is found to be thermodynamically stable up to 1100℃, t-ZrO_2 phase exists between 1100℃ to2370℃ and c-ZrO_2 phase exists at greater temperatures above 2370℃ [2]. The combination allows for the creation of crystal structures.

Barium can be used as a dopant in various materials to alter their properties in a specific ways to make them more suitable for various applications. Barium doping can modify the electrical conductivity of semiconductors. In cathode materials, barium oxide makes the electron to be emitted from the cathode surface. Barium can enhance the luminescent properties,optical properties, brightness and the efficiency. Also when barium is doped with optical materials it modifies its refractive index.

Using nanoparticles, nano filtration or another result of nanotechnology, many problems relating to the purity of the water can be better. One of the most important things is to create new technologies for producing pure water. Compared to materials with big scale, nanomaterials have a large surface area. To enhance their affinity with particular compounds, these materials can combine with various chemical groups [1-8].In the advanced oxidation process semiconductor hetrerogeneousphotocatalysis has enormous energy to remove organic contaminants in water and air.The formation of electron-hole couple occurs when the sun's energy or UV light strikes the nanoparticles. This process can only be accomplished when the incoming light or energy exceeds the band gap of the nanoparticles, which helps to initiate a redox potential.

The mechanismsof photodegradation vary depending on the type of material and its chemical composition. The material absorbs photons of light in visible region and in UV region, which provides the energy needed to initiate chemical reactions such as bond breaking, oxidation and cross-linking inside the molecular structure of the material. This photochemical reaction generates highly reactive species such as free radicals, excited states, singlet oxygen, etc. will react with neighbouring molecule. This photochemical reactions cause the formation of new chemical bonds, degradation of some functional groups and degradation of dye concentration. Thus, the materials experience changes in physical, thermal, optical and mechanical properties. These changes lead to discoloration, embrittlement, cracking, chalking and loss of strength or flexibility.

2. EXPERIMENTAL:

2.1 Chemicals:

Zirconium (IV) oxynitrate hydrate ($ZrN_2O_7.xH_2O$), Ammonia solution (NH_3), Barium chloride ($BaCl_2.2H_2O$), Rhodamine B dye and Ethanol.

2.2 Methods:

2.2.1 Co-precipitation Method:

The co-precipitation method is a chemical precipitation procedure that creates a mixed precipitate made up of two or more insoluble species that are extracted from solution at the same time. It is used to produce multi-component oxide ceramics. The majority of the precursors employed in this process are inorganic salts, such nitrate, sulfate, chloride etc., which are dissolved in water or any other appropriate medium to create an ion-clustered, homogenous solution. The salts are then forced to precipitate as hydroxides, oxalates or hydrous oxides by subjecting the solution to pH adjustment or evaporation. The concentration of salt, temperature, actual pH, and rate of pH change all affect the production and aggregation of nanoparticles. Post precipitation, the solid mass is gathered, cleaned, and then heated to the sample's boiling point in order to progressively dry it out. When the desired outcome is nanosized powders, the washing and drying processes used for co-precipitated hydroxides must be taken into consideration as they have an impact on the level of agglomeration in the final powder. In most cases, calcination is required to convert the hydroxide into crystalline oxides. The advantages of co-precipitation processes are the uniformity of component distribution, the relatively low reaction temperature, the small and homogeneous particle size with weakly agglomerated particles, and the low cost.

2.2.2 Photocatalytic Method:

Photocatalytic process is used for the removal of hazardous contaminants in water. In this process, the required energy of the light must be above the energy band gap of the catalyst. When light energy strikes the semiconductor material, electrons are excited from valence band of the semiconductor to conduction band. Therefore, electrons (e^-) in the conduction band and holes in valence band (h^+) are generated. These photogenerated charge carriers (e^-/h^+) start the photocatalytic process. The holes in valence band oxidize the organic content with water molecules to produce hydroxyl radicals (•OH). The excited electrons in conduction band reduce the oxygen molecules and create superoxide radicals ($\bullet O_2^-$).

Semiconductor + hv → $h^+ + e^-$

$h^+ + e^-$ → energy

$h^+ + H_2O \rightarrow \bullet OH + H^+$

$e^- + O_2 \rightarrow \bullet O_2^-$

How long the photocatalystgenerate longer-lived electrons and holes shows the efficiency of the photocatalyst which causes to the production of reactive free radicals. The material, its operational parameters (pH of solution, irradiation time, and the existence of holes), and the material's condition (powder form or immobilization on support) all affect the photocatalyst. The reduction process of oxygen and the oxidation dye molecules should occur simultaneously to get good photocatalytic degradation. Thus, the formation of electron in the conduction band will be reduced and less electron hole pair recombination.

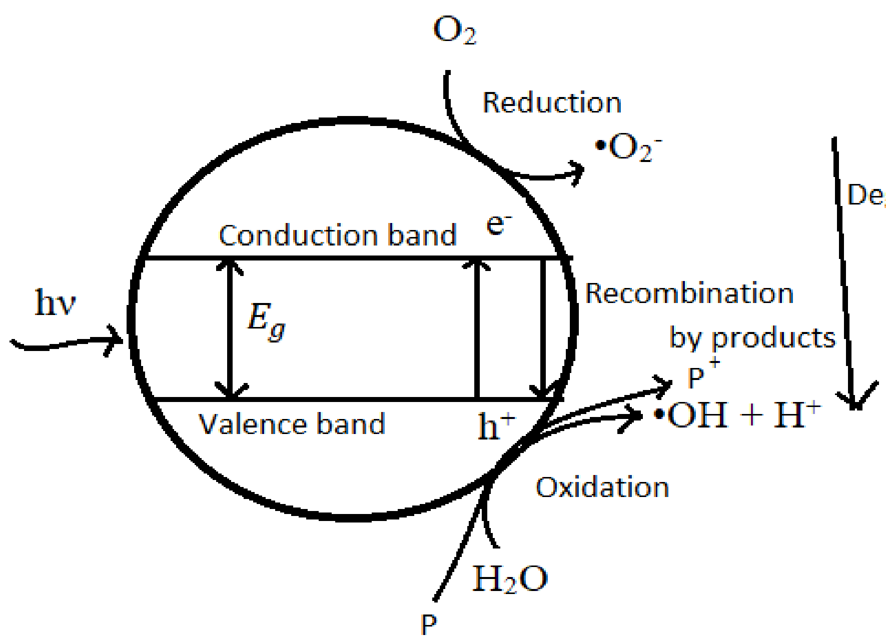

Figure: 1 Mechanism of electron – hole pair formation.

2.3Preparation of Zirconium Dioxide Nanoparticles by Co-precipitation Method:

Zirconium hydroxide was precipitated by adding drop-by-drop NH_3 aqueous solution to the$ZrN_2O_7.xH_2O$ aqueous solution at room temperature while rapidly stirring the mixture until the desired pH of 10 was attained. The subsequent stirring took place for two hours. The residue was washed with deionized water and ethanol before drying for two hours at 200°C. The desiccated zirconium hydroxide was then calcined at 600°C for two hours to produce undoped zirconium dioxide nanoparticles [9].

The subsequent procedures were used to prepare barium doped ZrO_2. In two different beakers, the aqueous solutions of 0.2 M $ZrN_2O_7.xH_2O$were taken. In those two distinct beakers, 0.02 M of 5% weight Barium chloride and 0.04 M of 10% weight barium chloride were added and vigorously stirred for two hours at room temperature. An aqueous solution of NH_3 was introduced drop by drop until the desired pH of 10 was achieved. The subsequent stirring took place for two hours. The precipitates were washed with deionized water before drying for two hours at 200°C. The barium doped zirconium dioxide nanoparticles werecalcined at 600°C for two hours. In this manner, samples of undopedZrO_2, 5% weight barium doped ZrO_2 and 10% weight barium doped ZrO_2 were produced.

3. RESULTS AND DISCUSSIONS:

The synthesized zirconium dioxide nanoparticles by co-precipitation method were characterized using various techniques such as Powder XRD, FTIR, UV-Visible spectroscopy, SEM, EDAX, Photoluminescence, Raman Spectroscopy and Photocatalytic Degradation.

3.1 X-RAY DIFFRACTION ANALYSIS:

The purity and crystallinity of the synthesized ZrO_2nanoparticles were examined by PXRD. The PXRD spectra for undoped and barium doped ZrO_2 nanoparticles are shown in the Figure: 2. Identification was done by comparing the diffraction patterns with the standard X-ray diffraction pattern of the ZrO_2 nanoparticles. It is inferred that the undoped and Ba doped ZrO_2 reveal the pure phase of the samples because the prominent peaks identified with the plane coincide with (PCPDF No. 79-1769) and no additional peaks associated with impurities are seen. In 10% Ba doped ZrO_2diffraction peak is more distorted than othersdue to the difference in ionic radii of dopant and atom in host lattice.All ZrO_2 peaks identify the tetragonal phase structure [10]. The following formula can be used to determine an average crystallite size (D).

Crystallite size $D = K\lambda / (\beta \cos \theta)$ (Scherrer's formula)

Where shape factor K=0.9, wavelength of the CuK radiation λ=0.1541 nm and β = Full Width Half Maximum of the diffracted peak are present and θ is the diffraction angle of the highest intensity peak. Table:1 displays the microstructural characteristics. At low temperatures, the crystallite size is an important factor in the creation of stabilized t-ZrO_2 and the doping of barium reduces crystallite size even more. The diffraction intensity is increased first and under a certain critical crystallite size, it is observed that the stability of tetragonal phase is more than a monoclinic phase and that as particle size declines, the surface energy to total energy ratio increases. According to experimental evidence from Ronald C. Garvie, the monoclinic phase is stable above 30 nm and the tetragonal phase is stable below 30 nm [10]. Thus the tetragonal phase is observed due to the crystallite size of the undoped and barium doped ZrO_2 nanoparticles [11, 26]. The calculated average crystallite sizes are 25.94 nm, 29.63 nm and 20.58 nm for undoped, 5% Ba doped ZrO_2 and 10% Ba doped ZrO_2 nanoparticles respectively.

The dislocation density $\delta = 1/D^2$

Here, D is the calculated crystallite size. Using the above equation, the dislocation densities are 0.001486, 0.001139 and 0.002361 for undoped, 5% Ba doped $ZrO_2$and 10% Ba doped ZrO_2 nanoparticles respectively.

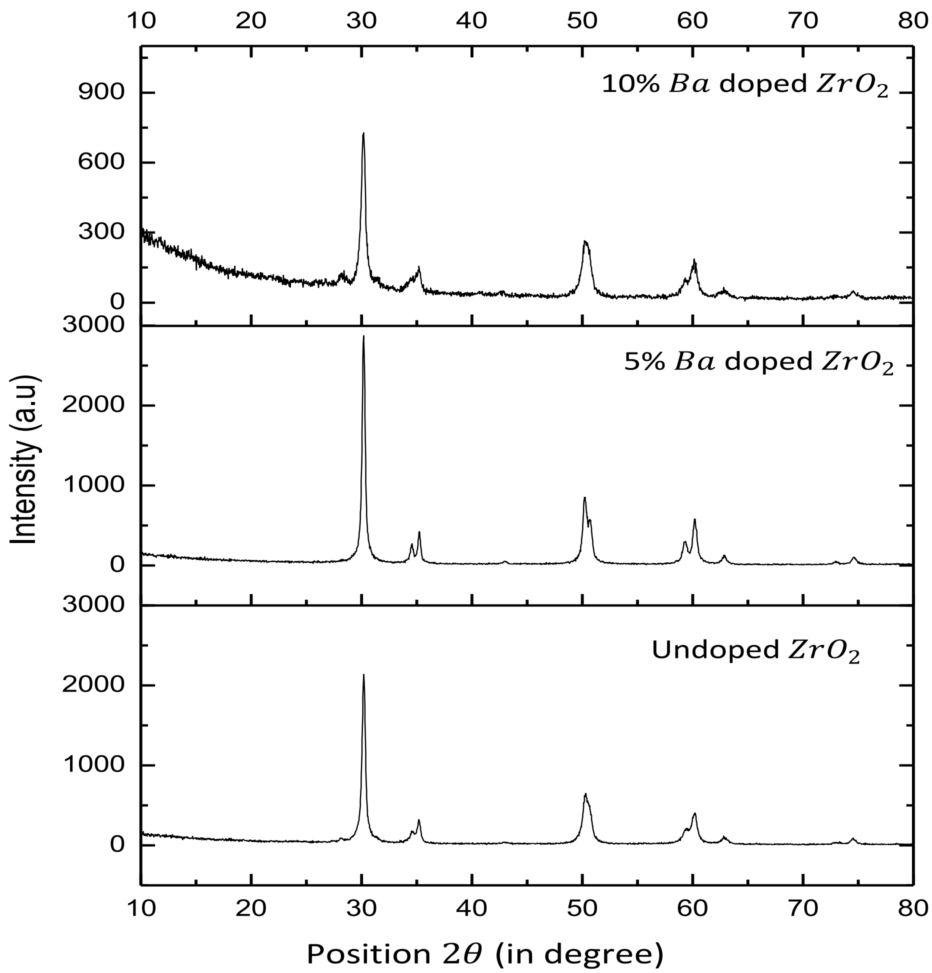

Figure: 2 The PXRD spectra for undoped and Ba doped ZrO_2 nanoparticles

Samples	Position $(2\theta)^0$	Lattice Constant Å			Miller indices (h k l)	Average crystallite size (nm)	Dislocation Density (δ)
		a	b	C			
UndopedZrO_2	30.1698	3.6062	3.6062	5.1841	1 0 1	25.94	0.001486
5% Ba doped ZrO_2	30.1621	3.6047	3.6047	5.184	1 0 1	29.63	0.001139
10% Ba doped ZrO_2	30.1331	3.59	3.59	5.16	1 0 1	20.58	0.002361

Table: 1 The Cell parameters, Miller indices and Crystallite sizes of undoped and Ba doped ZrO_2

3.2 THE FTIR ANALYSIS:

The presence of functional groups and crystal phase can be understand with the help of FTIR analysis. Figure:3 displays the FTIR spectra of Ba doped and undopedZrO_2 nanoparticles. The FTIR spectra of the prepared three samples are presented here. The wide bands around1040 cm^{-1} correspond to alkoxy stretching of C-O[19]. The peaks appeared at1384 cm^{-1}depicts to O=H bonding [10]. In undopedZrO_2, the peak observed at 435 cm^{-1}implies the presence of tetragonal ZrO_2[10]. The sharp peak observed at 1632 cm^{-1}represents to N-H bending vibration of ZrO_2[10].The peak at 3411 cm^{-1}indicates the O-H stretching vibration of ZrO_2 [15].In barium doped ZrO_2,the peaks at the region of 480 $cm^{-1}$and 492 cm^{-1}confirm the presence of Zr-O-Zr vibrations [18]. The peak attained at 2360 cm^{-1} corresponds to coupling and bending vibrations of –OH group of ZrO_2 [10]. The peak appeared at 1652 cm^{-1}attributes to N-H bending vibration of ZrO_2 [10]. The peak located at 3445 cm^{-1}depicts the O-H stretching vibration of ZrO_2 [10, 15, 18].

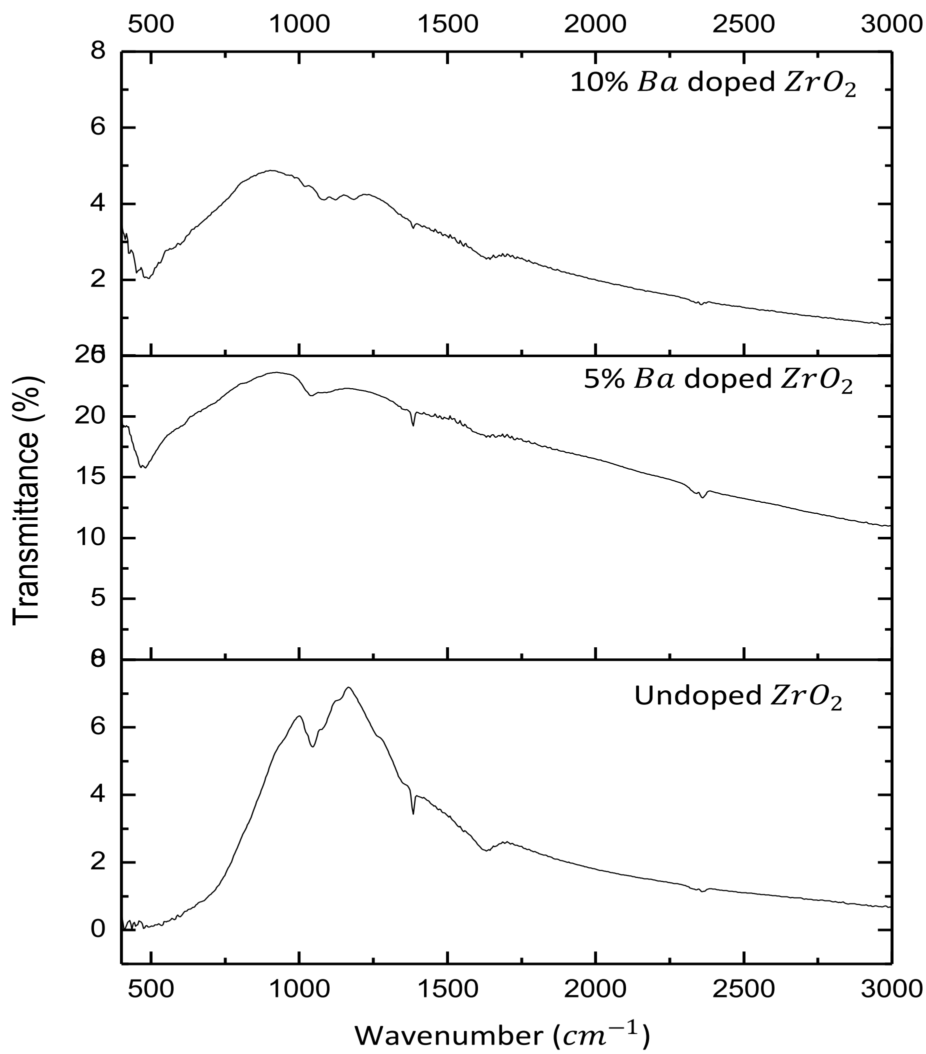

8049

Figure: 3 The FTIR spectra of undoped and Ba doped ZrO_2

3.3 SCANNING ELECTRON MICROSCOPY:

Scanning electron microscopy is used to examine the surface morphology of synthesized ZrO_2 nanoparticles that are both undoped and bariumdoped. Figures: 4(a),4(b) and 4(c) display the SEM pictures of undoped and Ba doped ZrO_2 nanoparticles respectively. It is observed that the synthesized samples are in fine spherical shape in the nano range. There are some bigger particles are in irregular cluster shapes as a result of the aggregation, merging or overlapping of smaller particles [10]. The Ba doped ZrO_2 particle size is smaller than the undopedZrO_2 due to the movement of crystallites is restricted at the contact on the boundaries between the two crystallite states [12,14,20].

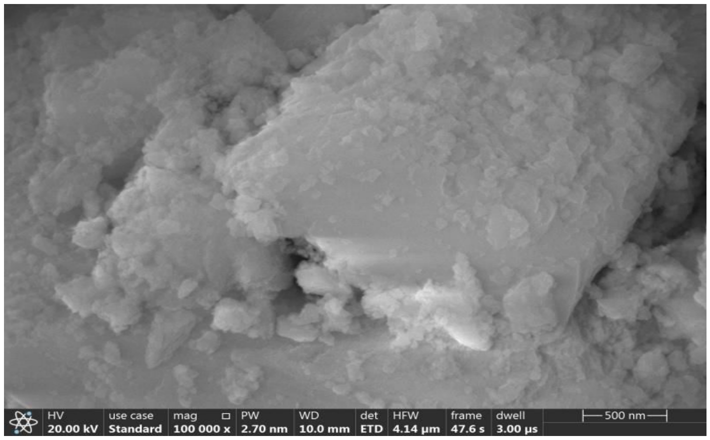

Figure: 4(a) SEM image of undopedZrO_2 nanoparticles

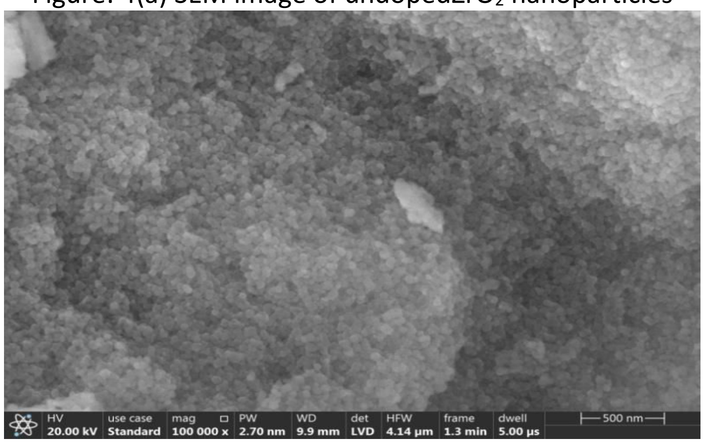

Figure: 4(b) SEM image of 5% Ba doped ZrO_2 nanoparticles

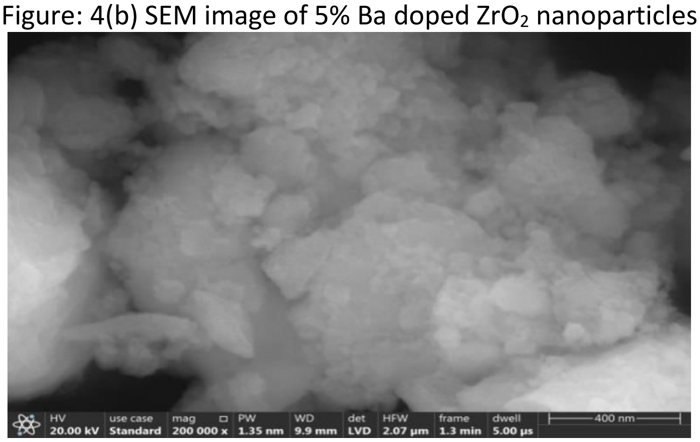

Figure:4(c) SEM image of 10% Badoped ZrO_2 nanoparticles

3.4 ELEMENTAL COMPOSITION (EDAX):

From EDAX analysis, Figures: 5(a), 5(b) and 5(c) shows the elemental composition of synthesized undoped and Ba doped ZrO_2 nanoparticles. Quantitative analysis was used to determine the structure and composition of crystalline ZrO_2 nanoparticles. The atomic percentage of elements present in

8050

undoped and Ba doped ZrO_2 nanoparticles showed the presence of Zr, O elementary species in the undopedZrO_2 nanoparticles in Table: 3(a) and the presence of Zr, O and Ba elementary species in the barium doped ZrO_2 nanoparticles in Table: 3(b) and 3(c), indicating the prepared sample's great purity and the absence of any other impurities [13,15,19].

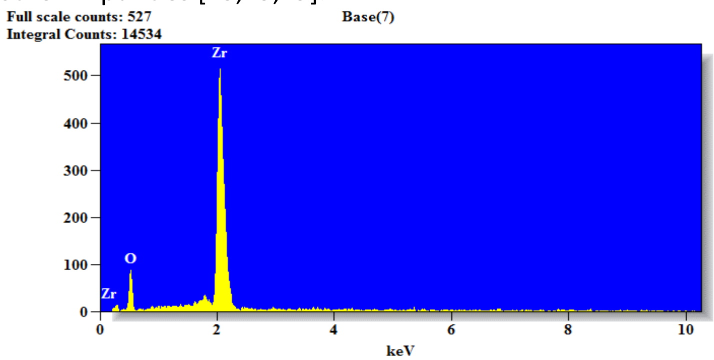

Figure: 5(a) EDAX image of undopedZrO_2 nanoparticles

Elements	Atomic Number	Net Counts	Weight (%)	Atom (%)
Zr	40	8211	70.23	29.27
O	8	549	29.77	70.73

Table: 3(a) Atomic percentage of elements present in undopedZrO_2 nanoparticles

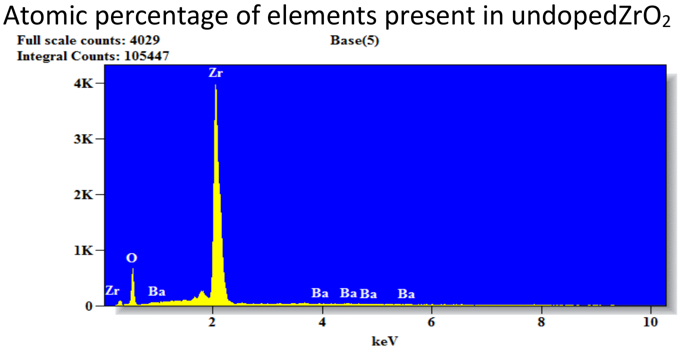

Figure: 5(b) EDAX image of 5% Ba doped ZrO_2 nanoparticles

Elements	Atomic Number	Net Counts	Weight (%)	Atom (%)
Zr	40	59062	71.96	31.51
O	8	3485	27.35	68.29
Ba	56	283	0.69	0.20

Table: 3(b) Atomic percentage of elements present in 5% Ba doped ZrO_2 nanoparticles

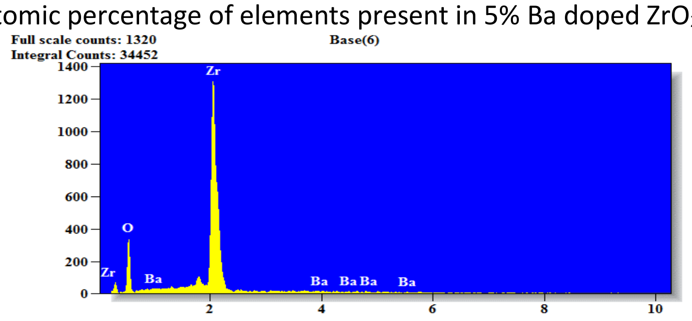

Figure: 5(c) EDAX image of 10% Ba doped ZrO_2 nanoparticles

8051

Elements	Atomic Number	Net Counts	Weight (%)	Atom (%)
Zr	40	18732	63.42	23.50
O	8	1845	36.16	76.40
Ba	56	63	0.42	0.10

Table: 3(c) Atomic percentage of elements present in 10% Ba doped ZrO_2 nanoparticles

3.5 RAMAN SPECTROSCOPY:

The Raman spectra of undoped and Badoped ZrO_2 nanoparticles are shown in Figure: 6. The Raman effect is based on the scattering of light. It is a non-destructive chemical analysis technique. The chemical structure, phase and polymorphy, molecular interactions and crystallinity of the prepared samples can be found using Raman Spectroscopy. The Raman bands of Ba doped and undopedZrO_2 nanoparticles are found to be intetragonal structure and the peaks are attributed at 145 $cm^{-1}$and 265 cm^{-1}respectively, while two additional bands reported for this structure at 314 $cm^{-1}$and 459 cm^{-1}appeared to coincide with monoclinic signals. The peak at 642 $cm^{-1}$is shared by tetragonal and monoclinic structures. Since the cubic structure of zirconia typically displays one distinct peak at 617 cm^{-1}, the lack of this signal indicates that only two structures (monoclinic and tetragonal) are present [18]. The peaks between 175 cm^{-1} to 194 cm^{-1} are very similar to those described for the monoclinic phase. The absence of this peak in 10% Ba doped ZrO_2 indicates that the monoclinic structure disappears as the barium doping concentration rises.

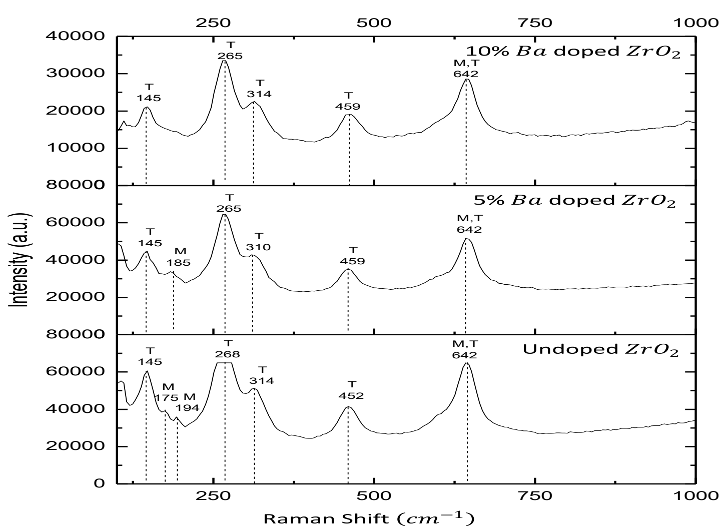

Figure: 6 Raman spectra of undoped and Ba doped ZrO_2 nanoparticles

3.6 THE UV-VISIBLE SPECTROSCOPY ANALYSIS:

Figure: 7(a) depicts the UV – Visible spectra of Badoped and undopedZrO_2 nanoparticles. The optical properties of the undoped and Badoped ZrO_2 nanoparticles are analysed. Intrinsic defects like vacancies, interstitial Zr and O vacancies are present in undopedZrO_2. Since they bring the donor or acceptor level in the bandgap, these inherent defects have a significant impact on ZrO_2's luminescent characteristics. The efficacy of optical and nanoelectronic devices using metaldoped ZrO_2 is observed to be improved [11, 12]. The optical absorbance rate was calculated using a 200–800 nm wavelength band. The valence to conduction band transition causes the UV spectra of undoped, 5% Ba doped and 10% Ba doped ZrO_2

nanoparticles to show absorption peaks at 262.5 nm, 260.8 nm and 258.5 nm respectively. There was a distinct absorption band in the UV region of the spectrum. This is due to charge transfer from oxygen to zirconium. InBa doped ZrO_2 nanoparticles, confinement of charge carriers is thecause of the blue shift in the absorption curve [14, 15, 16].

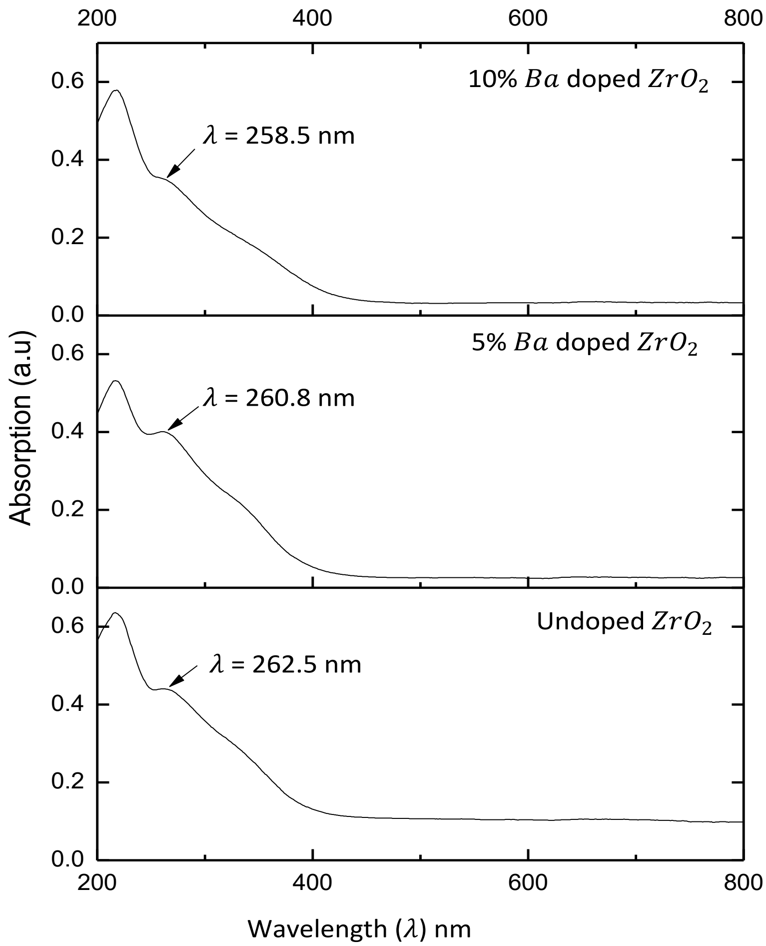

Figure: 7(a) The UV Absorption spectra of undoped and Ba doped ZrO_2

The Tauc's equation of $\alpha h\nu = (h\nu - E_g)^n$ can be used to determine the optical band gap of the nanoparticles, where n is the exponent factor determining the sort of transition causing the absorption and hv is the incident photon's energy, the value of n indicates the type of deal [21,22]. Depending on whether a transition is direct permitted, direct prohibited, indirect allowed, or indirect forbidden, it is interpreted as 1/2, 3/2, 2 or 3 [10, 16]. In Figure:7(b), the Tauc's relation is displayed. To calculate the optical band gap values of the undoped and Ba doped ZrO_2 nanoparticles, the experimental curves are matched with the straight line and were extended to cut off (hv) axis [25,26]. Undoped, 5% Ba and 10% Ba doped ZrO_2 nanoparticles have energy band gaps of 4.732eV, 4.764eV and 4.806eV, respectively. It was found that the optical band gap of 10% Ba doped ZrO_2 is slightly increased than the undoped and 5% Ba doped ZrO_2 nanoparticles [17].

8053

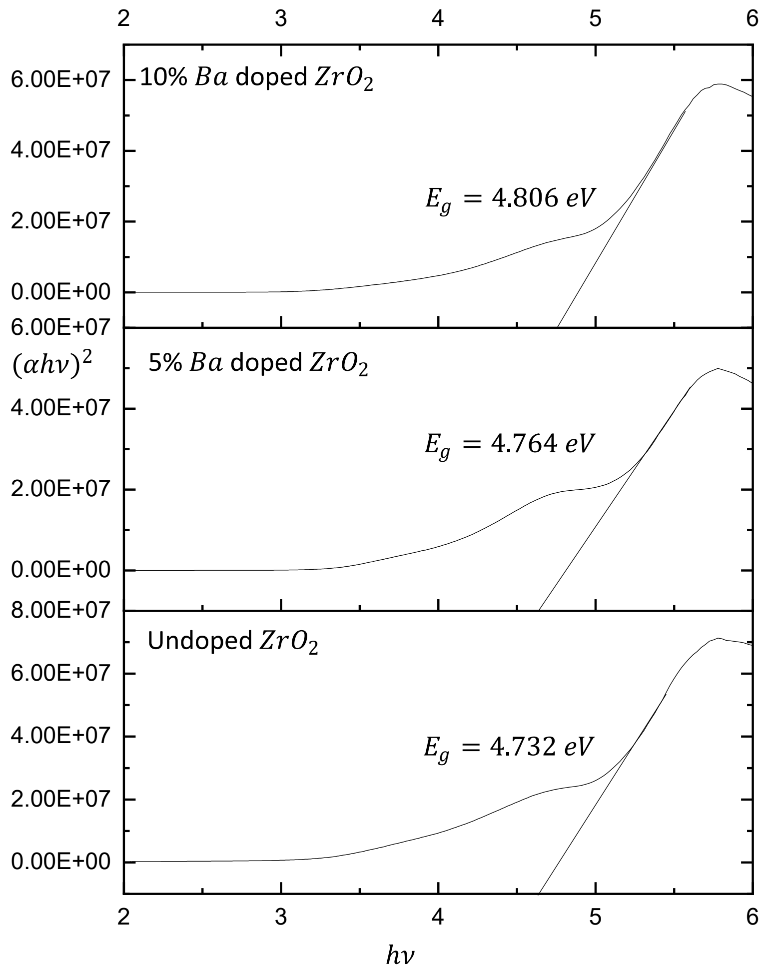

Figure: 7(b) The UV Tauc's plot of undoped and Ba doped ZrO_2

3.7 PHOTOLUMINESCENCE:

An important method for understanding electron-hole recombination process and the charge transfer over the photocatalytic substance is photoluminescence analysis [10]. New energy levels are formed on the surface of ZrO_2 as a result of electron transitions from the conduction to the valence band is generally the cause of ZrO_2's PL emission. Figure: 8 shows the Photoluminescence spectra of undoped and Ba doped ZrO_2.

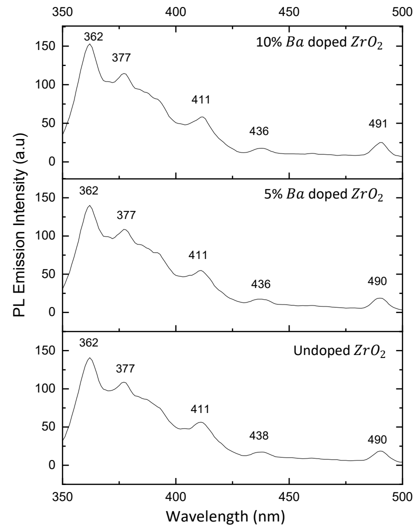

Figure:8 The Photoluminescence spectra of undoped and Ba doped ZrO_2

In every sample, at the emission peaks were obtained at 362 nm, 377 nm, 411 nm, 436 nm and 491 nm. These bands are thought to be the result of free-exciton recombination or band edge emission [12]. The mid-gap trap states, surface defects thought to be responsible for the 436 nm and 438 nm peaks. From PL analysis, the intensity of the PL emission spectra is decreased first and then increased when the concentration of the dopant is increased. It shows the more charge separation of electron-hole pairs. If the photoluminescence intensity will increase, the electron-hole pair recombination is high, the defects like dislocation is useful for oxygen transportation. The defects in the material depend on the density of defects in the materials and its temperature. If the PL emission intensity of the samples is decreased, the photocatalytic property of the samples will increase [21].

3.8 PHOTOCATALYTIC STUDIES:

An effective photogeneration of electrons and holes is necessary for excellent photocatalytic activity. The photo electron-holes generation is possible only when the energy gap of photon is greater than the energy gap of the photocatalyst. As sunlight has a continuous spectrum, if sunlight is the source, in a specific region of the spectrum, the large energy gap of catalyst will not be helpful for the generation of photoelectron-hole. Thus, the photocatalytic activity is increased due to the free electrons and holes [10].InUV visible spectroscopy, as the optical absorption of the prepared samples was exhibited in the ultraviolet region of 250 to 270 nm, the expected excellent photocatalytic degradation also will occur under UV light[12]. To avoid the recombination of photogenerated charge carriers, the oxygen vacancies on the surface can serve as photoinduced charge traps and adsorption sites [28]. Here, the charge can be transferred to the adsorbed molecules. The outcome is an increase in photocatalytic efficacy. The size, shape, crystal structure, and concentration of the composition of photocatalyst all affect the photocatalytic activity.

The degradation effectiveness of Rhodamine B under visible light (Philips, 40 W) and UV lightwere used to assess the photocatalytic activity of the substance. The mixed solution was magnetically stirred for 30 minutes in a dark chamber prior to the photocatalytic reaction to evenly distribute the catalyst. Additionally, it is made sure that the dye molecules attained a balance between adsorption and desorption on the catalyst surface. Under visible light and UV light, the combination underwent a photocatalytic process. Rhodamine B was made up to a quantity of 10 M. A UV-Vis spectrometer was used to determine the percentage of RhodamineB dye using a test wavelength of 558 nm. The degradation efficiency was calculated by,

Degradation percentage = $[(C_0 - C)/C_0]\times100$

Where, $C_0$is the initial concentration of aqueous solutionof dye andC is the concentration of aqueous solution of dye at a particular time. The absorbance occurred at 558 nm under visible light and UV light areshown in Figures:9(a) and 9(b) respectively.

Under visible light, the degradation percentage of the undopedZrO_2, 5% Ba doped $ZrO_2$and 10% Ba doped ZrO_2 are found to be 74.0%, 74.4% and 89.6% respectively. Under UV light, the degradation percentage of the undopedZrO_2, 5% Ba doped $ZrO_2$and 10% Ba doped ZrO_2 are found to be 82.8%, 92.4% and 96.0% respectively. According to the results, both undoped and Ba doped ZrO_2 catalysts have significantly good photocatalytic activity. The degradation percentage of the samples under UV light shows the better efficiency of the degradation of dye. The outcome also shows that while increasing the dopant concentration their photocatalytic activity also increases.

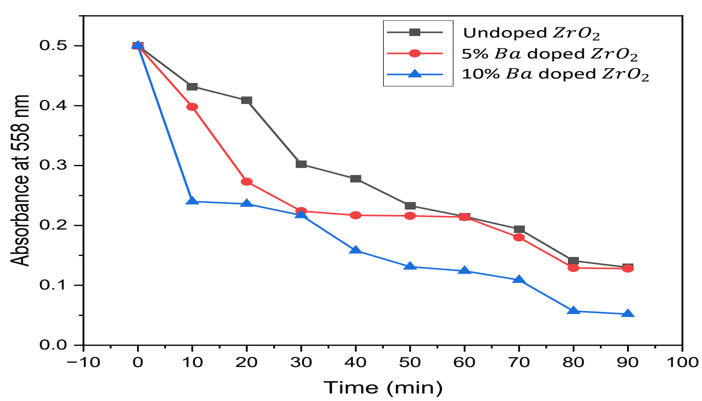

Figure: 9(a) Thephotocatalytic activity of undoped and Ba doped ZrO_2 under visible light.

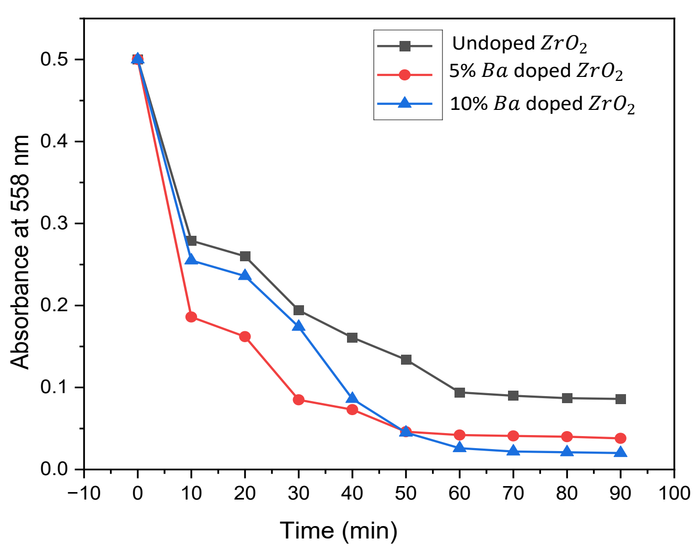

Figure:9(b)Thephotocatalytic activity of undoped and Ba doped ZrO_2 under UV light

The kinetics of the photodegradation $kt = (\ln C_0/C)$

Where k is the first-order kinetic constant and t is the duration of irradiation. The kinetic rate constants can be calculated by plotting ($\ln C_0/C$) with the irradiation time in hours. The Degradation rate comparison ofUndoped and Ba doped ZrO_2 under visible light and UV lightare shown in Figures:9(c) and 9(d) respectively. The percentage of degradation of dye under visible and UV light irradiation of undoped and barium doped ZrO_2 nanoparticles are displayed in Figure: 9(e).

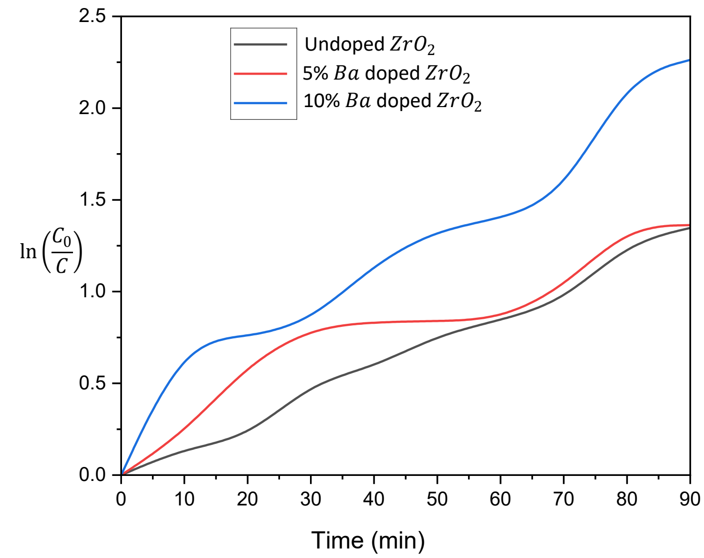

Figure: 9(c) The Degradation rate comparison ofundoped and Ba doped ZrO_2 under visible light

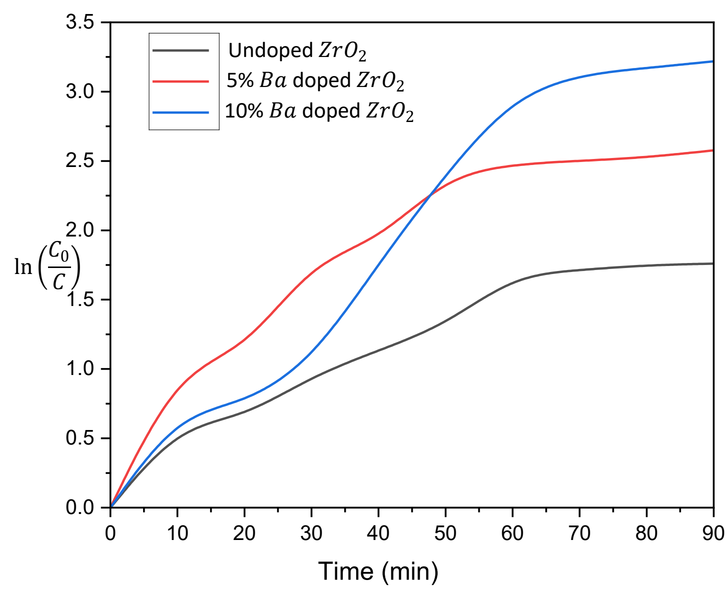

Figure: 9(d) The Degradation rate comparison ofundoped and Badoped ZrO_2 under UV light

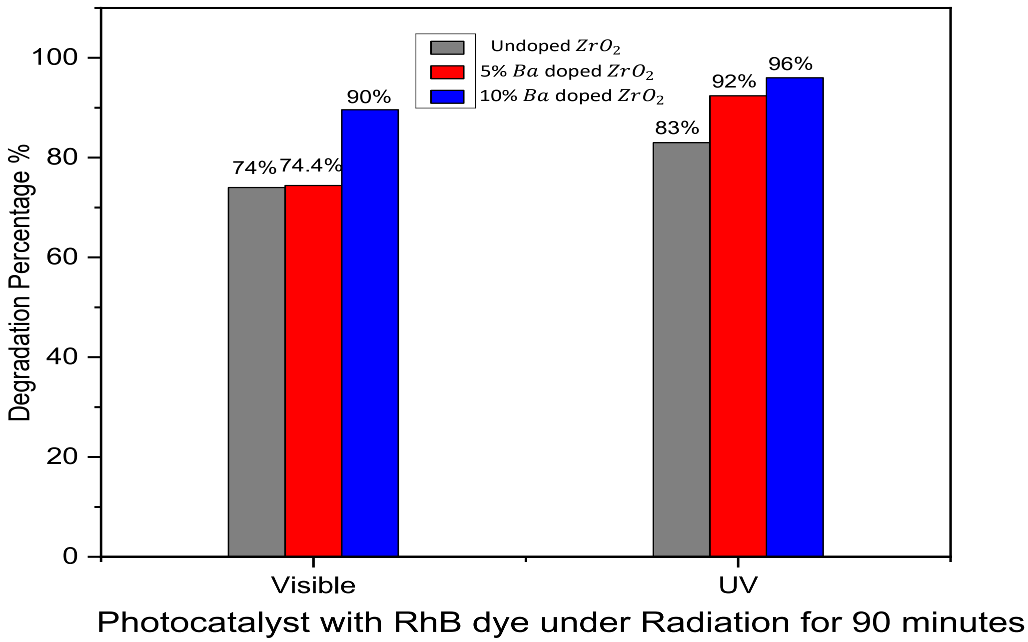

Figure: 9(e) The Percentage of Degradation under Visible and UV light of undoped and BA doped ZrO_2 nanoparticles

In Table:4 the percentages of the degradation efficiency signifies the undoped and doped metal oxides.

Photocatalyst	Light Source	Degradation Time (min)	Degradation Efficiency	Reference
Cu doped ZrO_2	UV Visible	120	85%, 96% and 100%	10
Fe doped ZrO_2	UV Visible	150	65%, 90% and 100%	11
Ce doped ZrO_2	Visible light	30	84%, 91% and 51%	27
ZnO - ZrO_2	UV Visible	120	74%, 50% and 5%	18
Zr doped CrO_2	UV Visible	140	50%, 64% and 37%	13
SiO_2TiO_2 : Sm^{3+}	UV Visible	90	85%, 70% and 95%	29
Ag doped ZrO_2	Visible light	180	74% and 96%	30
Ag doped ZnO	UV Visible	50	99% and 94%	31
Ba doped ZrO_2	Visible light UV Visible	90 90	74%, 74.4% and 89% 82.8%,92.4% and 96%	This work

Table: 4 Comparison of the results of photodegradation of the reportedphotocatalyst

4. SUMMARY AND CONCLUSION:

ZrO_2nanoparticles were successfully synthesized by co-precipitation method. The synthesized nanoparticles were analyzed using various characterization techniques. Their structural, morphological and optical properties were investigated.

The crystalline structure of the synthesized ZrO_2nanoparticles was determined by the Powder X-ray diffraction and the value of crystalline size was found by Scherrer's formula. From XRD pattern, the synthesizedZrO_2 nanoparticles are tetragonal in structure and the average crystalline size is 25.94 nm for undopedZrO_2, 29.63 nm for 5% Ba doped $ZrO_2$and 20.58 nm for 10% Ba doped ZrO_2nanoparticles.

The optical properties of the synthesized nanoparticles were studied using UV-Visible spectroscopy. From UV studies, the absorption spectra were obtained, from which cutoff wavelength is determined as 262.5 nm, 260.8 nm and 258.5 nm for undoped, 5% Ba doped ZrO_2 and 10% Ba doped ZrO_2 nanoparticles. The band gap energies were calculated using Tauc's plot as 4.732 eV, 4.764 eV and 4.806 eV for undoped, 5% Ba doped $ZrO_2$and 10% Ba doped ZrO_2 nanoparticles.

The surface morphologies of the synthesized nanoparticleswere analyzed using SEM images and are found to be in spherical shape and some irregular shape inthe nano range.

The compositionsof the elements in the synthesized nanoparticles were identified using EDAX spectrum. EDAX spectrum shows the presence of Zr, O and Ba elements with high purity in the prepared nanoparticles.

The functional group's presence in the samples were identified from FTIR spectroscopy. The peaks appeared at 480.87 cm^{-1} and 491.41 cm^{-1} correspond to Zr-O-Zr vibration and at 435.70cm^{-1} the peak depicts that the synthesized samples are in tetragonal structure.

From Raman spectroscopy the formation of tetragonal structure was observed.

The presence of defects and mechanism of recombination of the charge carrier are confirmed by photoluminescence spectra.

Under visible light, the percentage of degradation of the Rhodamine B dye of the undopedZrO_2, 5% Ba doped $ZrO_2$and 10% Ba doped ZrO_2 are found to be 74.0%, 74.4% and 89.6% respectively. Under UV light, the percentage of degradation of the Rhodamine B dye of the undopedZrO_2, 5% Ba doped $ZrO_2$and 10% Ba doped ZrO_2 are found to be 82.8%, 92.4% and 96.0% respectively. According to the results, both undoped and Ba doped ZrO_2 catalysts have significantly good photocatalytic activity while increasing the dopant concentration.The degradation percentage of the samples under UV light shows the better efficiency of the degradation of dye.

REFERENCES:

1. Mahdi Salehpour and FatemehGhanbary, [2016], "Synthesis of Cellulose/Zirconium oxide nanocompositeand the study of its activity in the removal of Pollutants", Salehpour and Ghanbary 2016, IIOABJ, Vol. 7, Suppl 5, 401-408.
2. Ayser S. Keiteb, Elias Saion, AzmiZakaria, and NayerehSoltani, [2016], "The structural and optical properties of zirconia nanoparticles by thermal treatment synthesis", Volume 2016, Article ID 1913609, 6 pages.
3. Anu Mary Ealias and Saravanakumar MP, [2017], "A review on the classification, characterization, synthesis of nanoparticles and their application", IOP Conf. Series: Materials Science and Engineering 263, 032019.
4. Vladimir Pokropivny, RynnoLohmus, Irina Hussainova, Alex Pokropivny, Sergey Vlassov, [2007], "Introduction to nanomaterials and nanotechnology", University of Tartu, 225, 978-9949-11-741-3.
5. Bharat Bhushan, [2010], "Springer handbook of nanotechnology", 3rd revised and extended edition, 1577 figures and 127 tables, 978-3-642-02524-2.
6. Charles P. Poole, [2003] "Introduction to nanotechnology", 1st Edition, 978-0471079354.
7. Suresh Sagadevan, JibanPodder and Isha Das, [2016], "The hydrothermal synthesis of zirconium oxide nanoparticles and its characterization", J Mater Sci: Mater Electron,10.1007/s10854-016-4469-6.
8. Tokeer Ahmed, MohdShahazad, Ruby Phul, [2017], "The hydrothermal synthesis of zirconia nanoparticles and its characterization and its dielectric

properties", Material Sci. & Eng. Int. J Volume 1 Issue 3, 100-104.

9. Rudzani A. Sigwadi, Sipho E. Mavundia, NosiphoMoloto, TouhamiMokrani, [2016], "The synthesis of zirconia-based solid acid nanoparticles for fuel cell application" Journal of Energy South Africa, Vol 27 No 2.
10. A. Arjun, AshwatiDharr, T. Raguram, K. S. Rajni, [2020], "Study of Copper Doped Zirconium Dioxide Nanoparticles Synthesized via Sol–Gel Technique for Photocatalytic Applications", Springer Science+Business Media, LLC, part of Springer Nature 2020, Journal of Inorganic and Organometallic Polymers and Materials.
11. YuanfengHui, Shuyue Zhang, [2021], "A Facile Synthesis of Fe-doped Zirconium Oxide Nanoparticles for Enhancement of Rhodamine B Dye Degradation", *Int. J. Electrochem. Sci.,* 16 (2021) Article ID: 210635.
12. Ali Fakhri, SajjadBehrouz, InderjeetTyagi, ShilpiAgarwal, Vinod Kumar Gupta, [2016], "Synthesis and characterization of ZrO_2 and carbon-doped nanoparticles for photocatalytic application", Journal of Molecular Liquids 216 (2016) 342–346.
13. Zahir Muhammad, Farman Ali, Muhammad Sajjad, Nisar Ali, Muhammad Bilal, Mohammed Rafi Shaik, Syed FarooqAdil, Mohammed A.F. Sharaf, EmadMahrousAwwad and Mujeeb Khan, [2021], "Zirconium-Doped Chromium IV Oxide Nanocomposites: Synthesis, Characterization, and Photocatalysis towards the Degradation of Organic Dyes", Catalysts 2021, 11, 117.
14. Mahwish Bashir, Robina Ashraf, Muhammad Imtiaz, SairaRiaz and ShahzadNaseem, [2013], "Synthesis and Characterization of ZrO_2 - ZnO Nanoparticles", Advances in nano, Biomechanics, Robotics, and Energy Research (ANBRE13), Seoul, Korea, August 25-28, 2013.
15. J. Chandradass, M. Balasubramanian& Ki Hyeon Kim, [2011], "Solution phase synthesis of t-ZrO_2 nanoparticles in ZrO_2–SiO_2 mixed oxide", Journal of Experimental Nanoscience, 6:1, 38-48.
16. Paolo Ghigna, Giorgio Spinolo, Umberto Anselmi-Tamburini, FilippoMaglia, Monica Dapiaggi, Gabriele Spina, and Luciano Cianchi, [1998], "Fe-Doped Zirconium Oxide Produced by Self-Sustained High-Temperature Synthesis: Evidence for an Fe-Zr Direct Bond", *J. Am. Chem. Soc., Vol. 121, No. 2, 1999.*
17. SanthoshBullapura Matt, Shivakumar. Manjunatha, S. Manjunatha, Dharmaprakash M. Sidlingappa, and ManjappaSidlingappa, [2019], "Synthesis of Cerium-Doped Zirconia Nanoparticles for the Electrochemical Detection of Dopamine by Modified Carbon Paste Electrode", Wiley-VCH Verlag GmbH & Co. KGaA, Weinheim, *Chemistry Select* 2019, *4*, 5839 –5844.
18. M. C. Uribe López,M. A. Alvarez Lemus,M. C. Hidalgo,R. López González,P. Quintana Owen,S. Oros-Ruiz,S. A. Uribe López,and J. Acosta, [2019], "Synthesis and Characterization of ZnO-ZrO_2Nanocomposites for Photocatalytic Degradation and Mineralization of Phenol", Hindawi Journal of Nanomaterials Volume 2019, Article ID 1015876, 12 pages.
19. T Mary Jeeva, J Judes and Sivakumar [2019], "Synthesis and characterization of metal-doped zirconia minispheres by sol-gel based freeze drying method", Mater. Res. Express 6 (2019) 105803.
20. Summaiyya Khan, Z. A. Ansari, H. K. Seo, and S. G. Ansari, [2018], "Synthesis and Application of Cu-Doped Nickel and Zirconium Oxide Nanoparticles as Brucellaabortus Electrochemical Device Development", American Scientific Publishers, Vol. 16, 267–276, 2018.

21. G. Viruthagiri, E. Gopinathan, N. Shanmugam, R. Gobi, [2014], "Synthesis and characterization of ZrO_2–CuO co-doped ceria nanoparticles via chemical precipitation method", SpectrochimicaActa Part A: Molecular and Biomolecular Spectroscopy 131 (2014) 556–563.
22. Islam MI Moustafaand Mohamed R Abdelhamid, [2018], "Synthesis of MgO-ZrO_2 Mixed Nanoparticles via Different Precursors: Identification of their Destructive Action for Organic Pollutants", Moustafa and Abdelhamid, et al., J ChemEng Process Technol 2018, 9:1.
23. Ayodeji Precious Ayanwale, Alvaro de Jes ´us Ru´ız-Baltazar, Le´on Espinoza-Crist ´ obal1, and Sim´onYobanny Reyes-L´opez1 [2020], "Bactericidal Activity Study of ZrO_2-Ag_2O Nanoparticles", Nanotechnology and Microtechnology in Drug Delivery System—Original Article, Dose-Response: An International Journal July-September 2020:1-13.
24. AmitSinghania and ShipraMital Gupta, [2017], "NanocrystallineZrO_2 and Pt-doped ZrO_2 catalysts for low-temperature CO oxidation, Beilstein Journal of Nanotechnology", 2017, *8,* 264–271.
25. Laura-Jayne A. Ellis, Anastasios G. Papadiamantis, StefanWeigel and Eugenia Valsami-Jones, [2018], "Synthesis and characterization of Zr- and Hf-doped nano-TiO_2 as internal standards for analytical quantification of nanomaterials in complex matrices", rsos.royalsocietypublishing.org *R. Soc. open sci.* 5: 171884.
26. L. Chouhan, G. Bouzerar, S.K. Srivastava, [2020], "d0 Ferromagnetism in Ag-doped monoclinic ZrO_2 compounds", hal-03011424.
27. PeishenLia, Ming Guoa, QiangWanga, Zhen Lia, ChangzhengWangb, Ning Chena, Chong-Chen Wangb, Chongqing Wana, ShaoweiChenc, [2019]. "Controllable synthesis of cerium zirconium oxide nanocomposites and their application for photocatalytic degradation of sulfonamides", Applied Catalysis B: Environmental 259 (2019) 118107.
28. Olga Długosz1, Krzysztof Szostak1, Marcin Banach1, [2019], "Photocatalytic properties of zirconium oxide–zinc oxide nanoparticles synthesised using microwave irradiation", Applied Nanoscience, 10.1007/s13204-019-01158-3.
29. Tong Wu, Jingyao Li, Meiqi Chang, Yanhua Song, Qi Sun, Fangke Wang, HaifengZou, Zhan Shi, [2020], " Photoluminescence properties and photocatalytic activities of SiO_2 @ TiO_2 : Sm^{3+}nanomaterials", Journal of Physics and Chemistry of Solids, 19 September 2020.
30. G. Murugadoss, D. Dinesh Kumar, M. Rajesh Kumar, N. Venkatesh, P. Sakthivel, [2021], "Silver decorated CeO_2 nanoparticles for rapid photocatalytic degradation of textile rose Bengal dye", scientific reports, nature research, (2021)11:1080.
31. Hyeonhan Lim, Mohammad Yusuf, Sehwan Song, SungkyunParkb and Kang Hyun Park, [2021], "Efficient photocatalytic degradation of dyes using photo-deposited Ag nanoparticles on ZnO structures: simple morphological control of ZnO", Royal Soceity of Chemistry, RSC Adv., 2021, 11, 8709.